Application of Ring-Closing Metathesis to Grb2 SH3 Domain-Binding Peptides

Fa Liu[†,*,§], **Alessio Giubellino**[‡], **Philip C. Simister**[¶], **Wenjian Qian**[†], **Michael C. Giano**[†], **Stephan M. Feller**[¶], **Donald P. Bottaro**[‡], and **Terrence R. Burke Jr.**[†,*]

[†]Chemical Biology Laboratory, Molecular Discovery Program, Center for Cancer Research, National Cancer Institute, National Institutes of Health, NCI-Frederick, Frederick, MD 21702

[‡]Urologic Oncology Branch, National Cancer Institute, National Institutes of Health, Bethesda, MD 20989

[¶]Cell Signalling Group, Weatherall Institute of Molecular Medicine, University of Oxford, Oxford OX3 9DS, UK

Abstract

Molecular processes depending on protein-protein interactions can utilize consensus recognition sequences that possess defined secondary structures. Left-handed polyproline II (PPII) helices are a class of secondary structure commonly involved with cellular signal transduction. However, unlike α-helices, for which a substantial body of work exists regarding applications of ring-closing metathesis (RCM), there are few reports on the stabilization PPII helices by RCM methodologies. The current study examined the effects of RCM macrocyclization on left-handed PPII helices involved with the SH3 domain-mediated binding of Sos1 to Grb2. Starting with the Sos1-derived peptide "Ac-V^1-P^2-P^3-P^4-V^5-P^6-P^7-R^8-R^9-R^{10}-amide", RCM macrocyclizations were conducted utilizing alkenyl chains of varying lengths originating from the pyrrolidine rings of the Pro^4 and Pro^7 residues. The resulting macrocyclic peptides showed increased helicity as indicated by circular dichroism and enhanced abilities to block Grb2-Sos1 interactions in cell lysate pull-down assays. The synthetic approach may be useful in RCM macrocyclizations where maintenance of proline integrity at both ring junctures is desired.

Keywords

peptide macrocyclization; ring-closing metathesis; polyproline type II helix; Grb2; Sos1; SH3 domain

INTRODUCTION

Stabilization of α-helices through ring closing metathesis (RCM) macrocyclization[1–6] has been shown to be impart biological advantages to certain peptides.[7, 8] Application of RCM macrocyclization to other classes of helices is less common, with stabilization of 3$_{10}$ helices being a rare example.[9, 10] Polyproline type II (PPII) helices represent physiologically important motifs that are characterized by an extended left-handed helical conformation having a translation of 3.12 Å per residue, trans-amide bonds, three residues per turn and typical backbone dihedral values $\phi - 75°$ and $\psi + 145°$.[11] PPII helices are widely involved in protein-protein interactions related to cellular signaling.[12–14] This is exemplified by the

---

[*]Corresponding Authors: To whom correspondence should be addressed. (F. L.): Tel. 317-651-9434, liu_fa_x1@lilly.com or (T. B.): Tel. 301-846-5906, tburke@helix.nih.gov.
[§]Currently with Lilly Research Laboratories, Indianapolis, IN 46285

growth factor receptor bound protein 2 (Grb2), which is composed of a central SH2 domain that recognizes phosphotyrosyl-containing sequences, flanked by amino- and carboxy-terminal SH3 domains that bind to PPII and 3_{10} helices.[15] Grb2 is a prototypical adaptor protein mediating receptor tyrosine kinase signaling, whose involvement in oncogenic pathways makes it a potential target for anticancer therapeutic development.[16, 17] Because inhibitors of SH3 domain binding may down-regulate Grb2 function, efforts have been undertaken to increase the effectiveness of SH3 domain-inhibitor interactions.[18–22] Artificial induction of PPII helices through non-covalent conformational stabilization has been reported using modified proline residues,[23–26] however, only a single example has been reported of an RCM approach to PPII stabilization, and in this case the requisite alkenyl chains were appended to peptide backbone amide nitrogens.[27] The objective of the current study was to examine the effects of RCM macrocyclization on Grb2 SH3 domain-binding peptides by employing alkenyl chains originating from the pyrrolidine rings of key proline residues.

RESULTS

Macrocycle Design

Two classes of binding modes (Class I and Class II) that differ on their binding orientations have been shown for the interaction of PPII helices with SH3 domains.[28] The Sos1-derived sequence, "Ac-V^1-P^2-P^3-P^4-V^5-P^6-P^7-R^8-R^9-R^{10}-amide" (**1**) has been shown to bind with high affinity to the Grb2 N-terminal domain SH3 domain and to bind to the SH3 C-terminal domain in a same orientation and mode, but with lower affinity.[29, 30] (The affinities for the C-terminal and N-terminal domains have been reported as 2.6 μM and 40 μM, respectively.)[31] NMR solution structures of **1** bound to the Grb2 N-terminal SH3 domain show the peptide binds in a Class II orientation with the region $\underline{\mathbf{P}}^3$-P^4-V^5-$\underline{\mathbf{P}}^6$-P^7-R^8 encompassing a prototypical PPII **Pro**-x-x-**Pro** motif, in which the $\mathbf{P}^3$, $\mathbf{V}^5$ and $\mathbf{P}^6$ residues bind in hydrophobic recognition pockets designated PIV, PII and PV, respectively (Figure 1).[28, 32] The neighboring P^4 and P^7 residues, which are situated one turn apart (approximately 9 Å) and lie on the side of the helix opposite to the protein-binding $\mathbf{P}^3$ and $\mathbf{P}^6$ residues, were chosen as sites for introduction of RCM ring-closing functionality (Figure 1).

Alkenyl ether groups were introduced at the P^4 and P^7 proline γ-methylenes (pyrrolidine C4). To minimize perturbation of the protein-bound helix geometry conformation, the alkenyloxy groups originate from the pyrrolidine rings of the P^4 and P^7 residues with (4S) and (4R) configurations, respectively (Figure 1). The distance between these positions in the protein-bound solution structure was calculated to be approximately 8.8 Å (Figure 1). However, because the optimal lengths for the ring-closing segments were not obvious, three macrocycles were prepared that contained ring-closing segments of increasing length, from four to six carbons. This required the synthesis of the N-Fmoc-protected proline analogues **2** and **3a – 3c** (Figure 2).

Macrocycle Synthesis

Solid-phase peptide synthesis was conducted on NovaSyn®TGR resin using standard Fmoc solid-phase protocols and active ester coupling. The alkenyloxy-containing proline analogues **2** and **3a – 3b** were employed to prepare the resin-bound metathesis precursors **4a – 4c**, respectively. Portions of the resins were cleaved to provide the corresponding open-chain peptides **5a – 5c** (Scheme 1). On-resin ring closure of **4a – 4c** was then conducted using Grubbs 2nd Generation[33] and the resulting peptide resins (**6a – 6c**) were cleaved by treatment with TFA and purified by HPLC to yield the final macrocyclic peptides **7a – 7c**

(Scheme 1). Scrambling of the wild-type peptide (WT) (**1**) provided Ac-P-R-V-P-P-P-P-V-R-R-NH$_2$ (**13**) as a negative control for binding experiments.

Determination of Grb2 SH3 N-domain Binding Affinities

Grb2 forms a complex with Sos1 through interactions of its C- and N-terminal SH3 domains with "P-x-x-P-x-R" sequences in Sos1, with the N-terminal SH3 domain-binding affinity of WT peptide **1** having been reported as K$_d$ = 39 µM by isothermal calorimetry.[32] In our current work, *in vitro* Grb2 SH3 N-domain binding affinities of synthetic peptides were determined using a Trp-fluorescence assay.[34] The WT peptide **1**, as well as the open-chain metathesis precursors **5a** – **5c**, showed similar binding affinities (K$_d$ ≈ 11 – 14 µM; Table 1). In comparison, the affinities of the macrocyclic peptides were lower and ranged from K$_d$ ≈ 33 µM for the smallest macrocycle (**7a**) to K$_d$ ≈ 18 µM for the largest macrocycle (**7c**), with the intermediate sized **7b** exhibiting K$_d$ ≈ 24 µM (Table 1).

Blockade of Grb2 – Sos1 Association in Cell Lysates

The peptides were also examined for their ability to block the binding of Sos1 to full-length Grb2. Non-ionic detergent lysates were prepared from human pheochromocytoma-derived PC12 cells, which express high levels of both Grb2 and Sos1.[35] Synthetic peptides at different concentrations were added to the lysates and measured for their ability to compete for Grb2 pull down using our recently reported biotinylated Grb2 capture reagent immobilized to streptavidin-coated microbeads.[36] This reagent binds selectively to the Grb2 SH2 domain with high affinity.[37] At 1 µM concentrations, the scrambled negative control peptide **13** showed little inhibition of Grb2-Sos1 association. In contrast, the WT peptide **1** and the open-chain RCM precursor peptide **5a** exhibited similar but modest inhibition (Figure 3). Relative to **1** and **5a**, the open-chain analogues **5b** and **5c** showed slightly higher inhibitory potencies. At 1 µM concentrations the macrocyclic peptides **7a** – **7c** were able to effectively block Grb2 – Sos1 interactions, while at 300 nM concentrations these peptides displayed clear differential inhibition, in the potency order: **7a** > **7c** > **7b** (Figure 3). At the lowest concentrations tested (100 nM), only **7a** showed visible inhibition. While the IC$_{50}$ values for **7b** and **7c** were in the range of 1 µM – 300 nM, the most effective analogue (**7a**) had an apparent IC$_{50}$ value between approximately 100 nM and 300 nM.

Examination of PPII Helicity Using Circular Dichroism

From the above data it was clear that introduction of alkenyloxy functionality modestly enhanced inhibitory potency, while macrocyclization resulted in significantly more effective binding antagonists. Evaluation of PPII helicity was undertaken by measuring circular dichroism (CD) peak intensities at 226 nm.[38] An overlay of linear and cyclic peptide spectra expanded about λ$_{226}$ showed that none of the linear peptides **5a** – **5c** or WT peptide **1** showed appreciable PPII helical character (Figure 4). All three of the macrocyclic peptides (**7a** – **7c**) showed slightly increased PPII helical character relative to the WT peptide **1** and open-chain metathesis precursors **5a** – **5c**.

In order to gain greater understanding of the effect of macrocyclization on PPII helical conformation, cryogenic studies were conducted by running far UV CD spectra of **7a** and the corresponding linear precursor **5a** at different temeratures in pH 7.4 PBS buffer, with and without detergent Triton X-100 (Figure 5). The changes in [θ]$_{max}$ = 226 nm as a function of temperature for peptides **5a** and **7a** in pH 7.4 PBS buffer without detergent were also plotted (Figure 6). Overall, the data indicated Triton X-100 did have some effects in disturbing the peptide solution conformation, and a negative correlation between molar ellipticity at 226 nm and temperature confirmed the existence of PPII helix. However the plot of the molar ellipticity of **5a** and **7a** at 226 nm against temperature indicated that

macrocyclization has minimal effects on the stability of PPII helical structure against increasing temperature.

DISCUSSION

In the *in-vitro* system with purified components, the addition of carbon macrocycles to the main peptide backbone (**7a – 7c**) has the effect of slightly reducing the binding affinity to the Grb2 SH3 N-domain relative to that of the WT Sos peptide (**1**). Linear peptides with uncoupled hydrocarbon chains display affinities equivalent to the WT peptide. A likely explanation for this observation is that the macrocyclic structures introduce constraint into the peptide backbone, resulting in a less flexible form or even a marginally altered structure compared to the WT peptide. This is consistent with the results of the circular dichroism analysis, which revealed a slightly higher helical content. Such a conformational difference, albeit minor, could impart different binding characteristics. Furthermore, with increasing macrocycle size, the binding affinity increases and approaches that of the wild-type peptide. Presumably this is related to a corresponding increased relaxation of the constraint imposed, as a function of macrocycle chain length. Finally, as the modified linear peptides (**5a – 5c**) would not be expected to constrain the native backbone configuration, they should not substantially alter the mode of docking (unless they hinder or enhance it somehow). This is reflected in their K_d values being similar to that of the WT Sos peptide (**1**).

The *in-vitro* fluorescence assay results, although internally consistent, are not in keeping with the competition assay using whole cell lysates, as revealed by Western blot analysis. Here the cyclic peptides at 1 μM concentration show a more potent inhibition of Sos binding. This could be due to the fact that the effective concentrations of peptides accessing the target may differ markedly between species. In addition, the affinities of the WT sequence and linear modified peptides for other SH3 domains present in the lysate may also be greater than those of the cyclized peptides, potentially leading to off-target binding that could reduce the available pool of peptide for specific Grb2 binding. It is also possible that the added hydrophobic character introduced by the hydrocarbon linker of the macrocyclic structures, could confer an increased tendency of these peptides to interact hydrophobic binding sites on the Sos protein substrate, thereby augmenting their inhibitory nature. The possibility of less specific binding by such hydrophobic structures is indicated by the fact that even the scrambled peptide (**13**) displays a low affinity for the Grb2 SH3 N-domain in the fluorescence assay. It should also be considered that differences in buffers used in assays could contribute to differences in apparent affinities. For example, the cell lysis buffer contains detergent unlike in the Trp-fluorescence assay, which may influence the solubility or aggregation state of either the peptide or proteins, and give rise to varying interaction behavior.

CONCLUSIONS

The current study represents only the second application of RCM macrocyclization to biologically active PPII helical peptides. The synthetic strategy employed is characterized by its use of proline γ-methylenes (pyrrolidine C4 positions) for introduction of ring-closing alkenyloxy functionality, with the locations of the ring-closing proline residues and the stereochemistry of the alkenyloxy substituents being based on the NMR solution structure of a linear WT peptide bound to the target Grb2 N-terminal SH3 domain protein. Alkenyloxy-substituted proline residues have been used for RCM macrocyclization onto alkenylglycine residues of random coil-constrained mimics of the membrane-proximal domain of FcεRIα.[38] Our current approach extends this technology by allowing RCM macrocyclization with maintenance of proline residues at both ring junctures. Within our

current system we have found that RCM macrocyclization can increase PPII helicity and enhance the ability of peptides to block Grb2 – Sos1 interactions.

MATERIALS AND METHODS

(2*S*,4*S*)-2-Allyl 1-*Tert*-butyl 4-(Allyloxy)pyrrolidine-1,2-dicarboxylate (9)

To a suspension of sodium hydride (60% in mineral oil, 380 mg, 9.50 mmol) in DMF (6 mL) at 0° C, was added a solution of (4*S*)-*N*-Boc- 4-hydroxy-L-proline (**8**, Scheme 2) (1.0 g, 4.32 mmol) [Sigma-Aldrich, Cat. 654019] in DMF (6 mL) dropwise (over 5 minutes). The mixture was kept at 0° C (15 minutes) then allylbromide (1.00 mL, 11.2 mmol) was added and the mixture was allowed to come to room temperature and stirred (overnight). The reaction was quenched by the addition of saturated aqueous NH_4Cl (50 mL) and extracted (EtOAc, 150 mL). The organic layer was washed, dried and purified silica gel chromatography (hexanes : EtOAc) to yield **9** (Scheme 2) as a colorless oil (1.25 g, 93% yield). ^{1}H NMR (400 MHz, CDCl$_3$) δ 5.87 – 5.71 (m, 2 H), 5.28 – 5.06 (m, 4 H), 4.60 – 4.45 (m, 2 H), 4.36 (dd, *J* = 8.4, 4.0 Hz, 0.4 H), 4.25 (dd, *J* = 8.4, 4.0 Hz, 0.6 H), 4.00 (m, 1 H), 3.87 – 3.82 (m, 2 H), 3.58 (dd, *J* = 7.6, 5.6 Hz, 0.6 H), 3.53 (dd, *J* = 7.6, 5.2 Hz, 0.4 H), 3.44 (dd, *J* = 7.6, 3.2 Hz, 0.6 H), 3.40 (dd, *J* = 7.6, 2.8 Hz, 0.4 H), 2.30 – 2.15 (m, 2 H), 1.40 (s, 3.5 H), 1.34 (s, 5.5 H). ^{13}C NMR (100 MHz, CDCl$_3$) δ 171.9, 171.5, 154.2, 153.8, 134.2, 132.0, 131.8, 118.4, 117.9, 116.8, 80.0, 76.6, 75.6, 69.7, 65.5, 57.7, 57.3, 51.9, 51.2, 36.1, 35.0, 28.3, 28.2. ESI (+VE) *m/z*: 334.4 (M + Na)$^+$.

(2*S*,4*S*)-1-((2-(9*H*-Fluoren-9-yl)ethoxy)carbonyl)-4-(allyloxy)pyrrolidine-2-carboxylic Acid [(4*S*)-*N*-Fmoc-4-allyloxyproline] (2)

A mixture **9** (Scheme 2, 1.25 g, 4.00 mmol) and LiOH monohydrate (336 mg, 8.00 mmol) in THF (5 mL) and H_2O (5 mL) was stirred at room temperature (3 h). Volatile organics were removed by rotary evaporation under reduced pressure and the aqueous phase was then washed (ether, 2 × 50 mL), acidified to pH 3 – 4 (1N aqueous HCl) and extracted (EtOAc, 150 mL). The EtOAc layer was washed, dried (NaSO$_4$) and evaporated to yield a colorless oil. This was treated with a mixture of TFA (10 mL) and dichloromethane (10 mL) (room temperature, 2 h). The solvent was removed by rotary evaporation under reduced pressure and the residue was placed under high vacuum (2 h) and then dissolved in dioxane (15 mL) and H_2O (15 mL). To this was added NaHCO$_3$ (1.68 g, 20 mmol) and Fmoc-OSu (1.52 g, 4.50 mmol), and the mixture was stirred (room temperature, overnight). Dioxane was removed by rotary evaporation under reduced pressure and the remaining aqueous phase was washed (ether, 50 mL × 2), acidified to pH 3 – 4 (1N aqueous HCl) and extracted (EtOAc, 200 mL). The organic layer was washed (brine), dried (NaSO$_4$) and evaporated to yield pure **2** as a white wax (1.52 g, 96% yield). ^{1}H NMR (400 MHz, CDCl$_3$) δ 11.0 (brs, 1 H), 7.73 (d, *J* = 7.6 Hz, 1 H), 7.68 (d, *J* = 7.6 Hz, 1 H), 7.62 – 7.53 (m, 2 H), 7.40 – 7.23 (m, 4 H), 5.80 (m, 1 H), 5.25 – 5.05 (m, 2 H), 4.54 – 4.45 (m, 2 H), 4.40 – 4.30 (m, 2 H), 4.23 (m, 0.5 H), 4.15 (m, 0.5 H), 4.08 (m, 0.5 H), 4.03 (m, 0.5 H), 3.89 (m, 1 H), 3.62 – 3.58 (m, 2 H), 2.40 (m, 1 H), 2.22 (m, 1 H). ^{13}C NMR (100 MHz, CDCl$_3$) δ 176.3, 175.8, 155.5, 155.0, 143.9, 143.6, 141.3, 134.0, 127.7, 127.1, 125.1, 125.0, 120.0, 117.1, 76.4, 75.5, 69.6, 67.9, 66.9, 57.8, 57.5, 52.2, 47.1, 36.0, 34.5. ESI (+VE) *m/z*: 416.2 (M + Na)$^+$. ESI-HRMS cacld for $C_{23}H_{24}NO_5^+$(M + H)$^+$: 394.1649, Found 394.1657.

(2*S*,4*R*)-1-((2-(9*H*-Fluoren-9-yl)ethoxy)carbonyl)-4-(allyloxy)pyrrolidine-2-carboxylic Acid [(4*R*)-*N*-Fmoc-4-allyloxyproline] (3a)

The synthesis of **3a** has been reported.[39]

(2*S*,4*R*)-4-(But-3-en-1-yloxy)-1-(*tert*-butoxycarbonyl)pyrrolidine-2-carboxylic Acid [(4*R*)-*N*-Boc-4-(but-3-en-1-yloxy)proline] (11)

A mixture of (4*R*)-*N*-Boc- 4-hydroxy-L-proline (**8**) (1.0 g, 4.32 mmol) [Sigma Aldrich: Cat. 518360] (2.0 g, 8.64 mmol), 4-bromo-1-butene (3.5 mL, 34.6 mmol) and potassium hydroxide (5 g) in a mixture of dioxane (5 mL) and H_2O (5 mL) was stirred room temperature, 48 h), acidified to pH 3 – 4 (1N aqueous HCl) and extracted (EtOAc). The organic layer was washed (brine), dried ($NaSO_4$) and evaporated to yield **11** (Scheme 2) as a colorless oil (100 mg). ^{1}H NMR (400 MHz, CDCl$_3$) δ 5.75 (m, 1 H), 5.07 - 4.99 (m, 2 H), 4.11 (dd, *J* = 8.0, 2.4 Hz, 0.6 H), 4.31 (t, *J* = 8.0 Hz, 0.4 H), 4.03 (m, 1 H), 3.58 (m, 1 H), 3.47 – 3.40 (m, 3 H), 2.36 (m, 1 H), 2.30 – 2.22 (m, 2 H), 2.21 – 2.05 (m, 1 H), 1.45 (s, 5.5 H), 1.39 (s, 3.5 H).

(2*S*,4*R*)-1-((2-(9*H*-Fluoren-9-yl)ethoxy)carbonyl)-4-(but-3-en-1-yloxy)pyrrolidine-2-carboxylic Acid Acid [(4*R*)-*N*-Boc-4-(but-3-en-1-yloxy)proline] (3b)

A solution of **11** (100 mg) in TFA (3 mL) and dichloromethane (3 mL) was stirred (room temperature, 2 h). The solvent was removed by rotary evaporation under reduced pressure and the residue was placed under high vacuum (2 h) and then dissolved in dioxane (3 mL) and H_2O (3 mL). To this was added $NaHCO_3$ (353 mg, 4.2 mmol) and Fmoc-OSu (142 mg, 0.42 mmol), and the mixture was stirred (room temperature, overnight). Dioxane was removed by rotary evaporation under reduced pressure and the remaining aqueous phase was washed (ether, 30 mL × 2), acidified to pH 3 – 4 (1N aqueous HCl) and extracted (EtOAc, 100 mL). The organic layer was washed (brine), dried ($NaSO_4$) and evaporated to yield pure **3b** (Scheme 2) as a white wax (140 mg, 98% yield). ^{1}H NMR (400 MHz, CDCl$_3$) δ 9.40 (brs, 1 H), 7.75 (d, *J* = 7.6 Hz, 1 H), 7.67 (d, *J* = 7.6 Hz, 1 H), 7.57 – 7.48 (m, 2 H), 7.40 – 7.23 (m, 4 H), 5.77 (m, 1 H), 5.10 – 4.99 (m, 2 H), 4.50 – 4.22 (m, 4 H), 4.10 (m, 1 H), 3.70 – 3.57 (m, 2 H), 3.47 – 3.37 (m, 2 H), 2.45 – 2.00 (m, 4 H). ^{13}C NMR (100 MHz, CDCl$_3$) δ 177.6, 176.3, 155.7, 154.7, 143.7, 141.3, 134.7, 127.7, 127.1, 125.0, 120.0, 116.7, 76.9, 76.2, 68.6, 67.9, 67.8, 58.0, 57.5, 51.9, 51.7, 47.1, 47.0, 36.8, 35.1, 34.1. ESI (+VE) *m/z*: 430.2 $(M + Na)^+$. ESI-HRMS cacld for $C_{24}H_{26}NO_5^+(M + H)^+$: 408.1806, Found, 408.1811.

(2*S*,4*R*)-1-((2-(9*H*-Fluoren-9-yl)ethoxy)carbonyl)-4-(pent-4-en-1-yloxy)pyrrolidine-2-carboxylic Acid [(4*R*)-*N*-Boc-4-(pent-4-en-1-yloxy)proline] (3c)

The synthesis of **3c** has been reported.[39]

Peptide Synthesis

Peptides were synthesized on NovaSyn®TGR resin (Novabiochem, cat. no. 01-64-0060) by standard Fmoc solid-phase protocols using active ester coupling (1-hydroxybenzotriazole (HOBT) and *N, N´*-diisopropylcarbodiimide (DIC) as coupling reagents (single couple, 2 hours). The guanidine functionality of arginine was protected using the 2,2,4,6,7-pentamethyldihydrobenzofuran-5-sulfonyl (Pbf) group. On resin ring-closing metathesis was conducted using dried resin (200 mg) mixed with anhydrous dichloromethane (3 mL) and de-gassed under argon (3 minutes). Grubbs 2nd Generation Catalyst [benzylidene[1,3-bis(2,4,6-trimethylphenyl)-2-imidazolidinylidene]dichloro(tricyclohexylphosphine) ruthenium][33] (15 mg) in anhydrous dichloromethane (4 mL) DCM) was added, and the mixture was agitated in a sealed (room temperature, 24 h). The resulting resin was washed with *N, N*-dimethylformamide, methanol, dichloromethane and ether and then dried under vacuum (overnight). Peptides were cleaved from resin (200 mg) by treatment with TFA: triisopropylsilane : H_2O (90 : 5 : 5) (5 mL, 4 h). The resin was removed by filtration and the filtrate was concentrated under vacuum, then precipitated with ether and the precipitate washed with ether. The resulting solid was dissolved in 50% aqueous acetonitrile (5 mL)

and purified by reverse phase preparative HPLC using a Phenomenex C_{18} column (21 mm dia × 250 mm, cat. no: 00G-4436-P0) with a linear gradient from 0% aqueous acetonitrile (0.1% TFA) to 65% acetonitrile (0.1% TFA) over 30 minutes at a flow rate of 10.0 mL/minute (detection at 220 nm). Lyophilization provided products as white powders. Mass spectral data are provided in Table 2.

Determination of Grb2 SH3 N-Domain-Binding Constants

Purification of Grb2 SH3-N domain—GST-Grb2SH3N fusion protein was expressed in *E. coli* strain BL21(DE3) from the pGEX-2T vector by inducing cultures overnight at 20°C with 50 μM IPTG. Cells were lysed by sonication in TPE lysis buffer (1% Triton X-100, PBS and 100 mM EDTA) with a protease inhibitor cocktail added. Insoluble material was centrifuged at 48,000 g for 1 hour and the soluble fraction was incubated overnight with glutathione sepharose beads. The next day beads were washed extensively with cold wash buffer (50 mM Tris pH 7.5, 100 mM EDTA, 0.1% Tween20) before overnight incubation with elution buffer (100 mM reduced glutathione brought to pH 8.0 with a concentrated Tris buffer stock). The eluted GST-Grb2SH3N was dialysed against 5 mM Tris pH 7.5 and then cleaved for 24 hours by incubation with thrombin protease before final purification using size exclusion chromatography (Superdex 75 column, GE Healthcare) in gel filtration buffer (20 mM Tris pH 7.5, 150 mM NaCl, 1 mM DTT). Purified Grb2 SH3-N domain was concentrated to give a stock of >1 mM.

Intrinsic tryptophan fluorescence measurements—Tryptophan fluorescence measurements to determine peptide-binding affinities were carried out with a Perkin Elmer LS50B spectrofluorimeter essentially as described previously.[34] Briefly, the excitation wavelength employed was 295 nm and the emission wavelength was 342 nm, at the maximum fluorescence intensity, using excitation and emission slit widths, respectively, set to 5 and 15 nm. Titration experiments, each in triplicate, were performed in filtered, degassed PBS buffer containing 1 mM DTT and the purified Grb2 SH3-N domain (6 μM) with continual stirring. The cuvette was maintained at a constant 21°C in its holder by a cycling water-cooling system linked to a thermostat-controled water bath. Peptides were titrated in until no increase in the fluorescence intensity was observed, typically giving 12 to 15 data points per experiment. A single-site binding model enabled an accurate curve to be fit to the data using Origin (v5.0) software, from which mean K_d values and standard deviations could be determined. Data is shown in Table 1.

Inhibition of Grb2 – SOS1 Association in Cell Lysates

Peptides were evaluated for their ability to block Grb2 – Sos1 binding interactions in cell lysates. Non-ionic detergent lysates were prepared from human pheochromocytoma-derived PC12 cells as described.[35] The detergent used was Triton X-100 (1%) and the composition of the buffer is as follow: Cell lysis buffer 100 mL: 1.2 g HEPES or 10 mL 500 mM HEPES (50 mM final), 0.4 g NaF, 0.05 g Na_3VO_4 (sodium orthovanadate, high purity), 0.45 g Na_4PO_2 (sodium pyrophosphate), 4 mL of 100 mM EDTA (4 mM final) and 10 mL 10% Triton X-100 (TX-100; high purity, Pierce). These cells were selected because they contain relatively high levels of both Grb2 and Sos1. SH3 domain binding antagonists were added to the lysates at the indicated concentrations together with a biotinylated Grb2 capture reagent that had been immobilized to streptavidin-coated microbeads.[36] The synthetic biotinylated Grb2 capture reagents binds selectively to the Grb2 SH2 domains with high affinity.[37] After 1 hour, the beads were removed by centrifugation, washed 3 times with lysis buffer [50 mM HEPES pH 7.4, 5 mM NaF, 1 mM Na_3VO_4, 4 mM EDTA, 5 mM Na_4PO_2, 1% Triton X-100, 1 mM phenylmethylsulfonyl fluoride, 1 ug/mL aprotinin] and bound proteins were extracted with boiling Laemmli buffer. Samples were resolved by reducing SDS-PAGE, electrophoretically transferred to PVDF membranes and immuno-detected using primary

antibodies for Sos1 (Millipore Corp.) or Grb2 (Santa Cruz Biotechnology) and secondary detection reagents for chemiluminescence. Results are shown in Figure 3.

CD Spectral Data

CD spectra of peptides **1**, **5a – 5c** and **7a – 7c** were collected on a Circular Dichroism Spectrometer AVIV Model 202 at 200 μM concentration in H_2O, pH 7.4 PBS buffer, and pH 7.4 PBS buffer with 0.1% Triton X-100. The CD spectrum at each condition was collected three times independently; the final plot was based on the average data of three independent runs. The spectrum of Ac-P-P-P-P-P-P-P-R-R-amide (**12**) is included as a reference exhibiting PPII helicity in solution. Results are shown in Figures 4 – 6.

Acknowledgments

References

1. Schafmeister CE, Po J, Verdine GL. J Am Chem Soc. 2000; 122:5891–5892.

2. Walensky LD, Pitter K, Morash J, Oh KJ, Barbuto S, Fisher J, Smith E, Verdine GL, Korsmeyer S. J Mol Cell. 2006; 24:199–210.

3. Bernal F, Tyler AF, Korsmeyer SJ, Walensky LD, Verdine GL. J Am Chem Soc. 2007; 129:2456–2457. [PubMed: 17284038]

4. Henchey LK, Jochim AL, Arora PS. Curr Opin Chem Biol. 2008; 12:692–697. [PubMed: 18793750]

5. Wang D, Lu M, Arora PS. Angew Chem Int Ed. 2008; 47:1879–1882.

6. Kutchukian PS, Yang JS, Verdine GL, Shakhnovich EI. J Am Chem Soc. 2009; 131:4622–4627. [PubMed: 19334772]

7. Wang D, Liao W, Arora PS. Angew Chem Int Ed. 2005; 44:6525–6529.

8. Arora PS, Ansari AZ. Nature. 2009; 462:171–173. [PubMed: 19907487]

9. Chapman R, Kulp JL III, Patgiri A, Kallenbach NR, Bracken C, Arora PS. Biochemistry. 2008; 47:4189–4195. [PubMed: 18335996]

10. Jacobsen O, Klaveness J, Ottersen OP, Amiry-Moghaddam MR, Rongved P. Org Biomol Chem. 2009; 7:1599–1611. [PubMed: 19343246]

11. Kapitán J, Gallo D, Goasdoué N, Nicaise M, Desmadril M, Hecht L, Leclercq G, Barron LD, Jacquot Y. J Pep Sci. 2009; 15:455–464.

12. Jacobsen O, Klaveness J, Rongved P. Molecules. 2010; 15:6638–6677. [PubMed: 20877250]

13. Siligardi G, Drake AF. Biopolymers. 1995; 37:281–292. [PubMed: 7540055]

14. Kay BK, Williamson MP, Sudol P. FASEB J. 2000; 14:231–241. [PubMed: 10657980]

15. Harkiolaki M, Tsirka T, Lewitzky M, Simister PC, Joshi D, Bird LE, Jones EY, O'Reilly N, Feller SM. Structure. 2009; 17:809–822. [PubMed: 19523899]

16. Dharmawardana PG, Peruzzi B, Giubellino A, Burke TR Jr, Bottaro DP. Anti-Cancer Drugs. 2005; 17:13–20. [PubMed: 16317285]

17. Giubellino A, Burke TR Jr, Bottaro DP. Exp Opin Therap Targ. 2008; 12:1021–1033.

18. Kardinal C, Konkol B, Lin H, Eulitz M, Schmidt EK, Estrov Z, Talpaz M, Arlinghaus RB, Feller SM. Blood. 2001; 98:1773–1781. [PubMed: 11535511]

19. Lewitzky M, Kardinal C, Gehring NH, Schmidt EK, Konkol B, Eulitz M, Birchmeier W, Schaeper U, Feller SM. Oncogene. 2001; 20:1052–1062. [PubMed: 11314042]

20. Feller SM, Lewitzky M. Curr Pharm Des. 2006; 12:529–548. [PubMed: 16472145]

21. Gril B, Vidal M, Assayag F, Poupon M-F, Liu W-Q, Garbay C. Int J Cancer. 2007; 121:407–415. [PubMed: 17372910]

22. Ye Y-B, Lin J-Y, Chen Q, Liu F, Chen H-J, Li J-Y, Liu W-Q, Garbay C, Vidal M. Biochem Pharmacol. 2008; 75:2080–2091. [PubMed: 18455151]

23. Ruzza P, Siligardi G, Donella-Deana A, Calderan A, Hussain R, Rubini C, Cesaro L, Osler A, Guiotto A, Pinna LA, Borin G. J Peptide Sci. 2006; 12:462–471. [PubMed: 16506148]

24. Jacquot Y, Broutin I, Miclet E, Nicaise M, Lequin O, Goasdoue N, Joss C, Karoyan P, Desmadril M, Ducruix A, Lavielle S. Bioorg Med Chem. 2007; 15:1439–1447. [PubMed: 17113302]

25. Flemer S, Wurthmann A, Mamai A, Madalengoitia JS. J Org Chem. 2008; 73:7593–7602. [PubMed: 18754643]

26. Tuchscherer G, Grell D, Tatsu Y, Durieux P, Fernandez-Carneado J, Hengst B, Kardinal C, Feller S. Angew Chem Int Ed. 2001; 40:2844–2848.

27. Liu F, Stephen AG, Waheed AA, Freed EO, Fisher RJ, Burke TR Jr. Bioorg Med Chem Lett. 2010; 20:318–321. [PubMed: 19914066]

28. Simon J, Schreiber SL. Chem Biol. 1995; 2:53–60. [PubMed: 9383403]

29. Yuzawa S, Yokochi M, Hatanaka H, Ogura K, Kataoka M, Miura K-i, Mandiyan V, Schlessinger J, Inagaki F. J Mol Biol. 2001; 306:527–537. [PubMed: 11178911]

30. McDonald Caleb B, Seldeen Kenneth L, Deegan Brian J, Farooq A. Biochemistry. 2009; 48:4074–4085. [PubMed: 19323566]

31. Cussac D, Vidal M, Leprince C, Liu W-Q, Cornille F, Tiraboschi G, Roques BP, Garbay C. Faseb J. 1999; 13:31–38. [PubMed: 9872927]

32. Wittekind M, Mapelli C, Lee V, Goldfarb V, Friedrichs MS, Meyers CA, Mueller L. J Mol Biol. 1997; 267:933–952. [PubMed: 9135122]

33. Kingsbury JS, Harrity JPA, Bonitatebus PJ, Hoveyda AH. J Am Chem Soc. 1999; 121:791–799.

34. Posern G, Zheng J, Knudsen BS, Kardinal C, Muller KB, Voss J, Shishido T, Cowburn D, Cheng G, Wang B, Kruh GD, Burrell SK, Jacobson CA, Lenz DM, Zamborelli TJ, Adermann K, Hanafusa H, Feller SM. Oncogene. 1998; 16:1903–1912. [PubMed: 9591773]

35. Atabey N, Gao Y, Yao Z-J, Breckenridge D, Soon L, Soriano JV, Burke TR Jr, Bottaro DP. J Biol Chem. 2001; 276:14308–14314. [PubMed: 11278639]

36. Shi Z-D, Liu H, Zhang M, Worthy KM, Bindu L, Yang D, Fisher RJ, Burke TR Jr. Bioor Med Chem. 2005; 15:4200–4208.

37. Giubellino A, Shi Z-D, Miller Jenkins LM, Worthy KM, Bindu LK, Athauda G, Peruzzi B, Fisher RJ, Appella E, Burke TR Jr, Bottaro DP. J Med Chem. 2008; 51:7459–7468. [PubMed: 18989951]

38. Helbecque N, Loucheux-Lefebvre MH. Int J Peptide Protein Res. 1982; 19:94–101. [PubMed: 7118386]

39. Peters C, Bacher M, Buenemann CL, Kricek F, Rondeau JM, Weigand K. ChemBioChem. 2007; 8:1785–1789. [PubMed: 17828717]
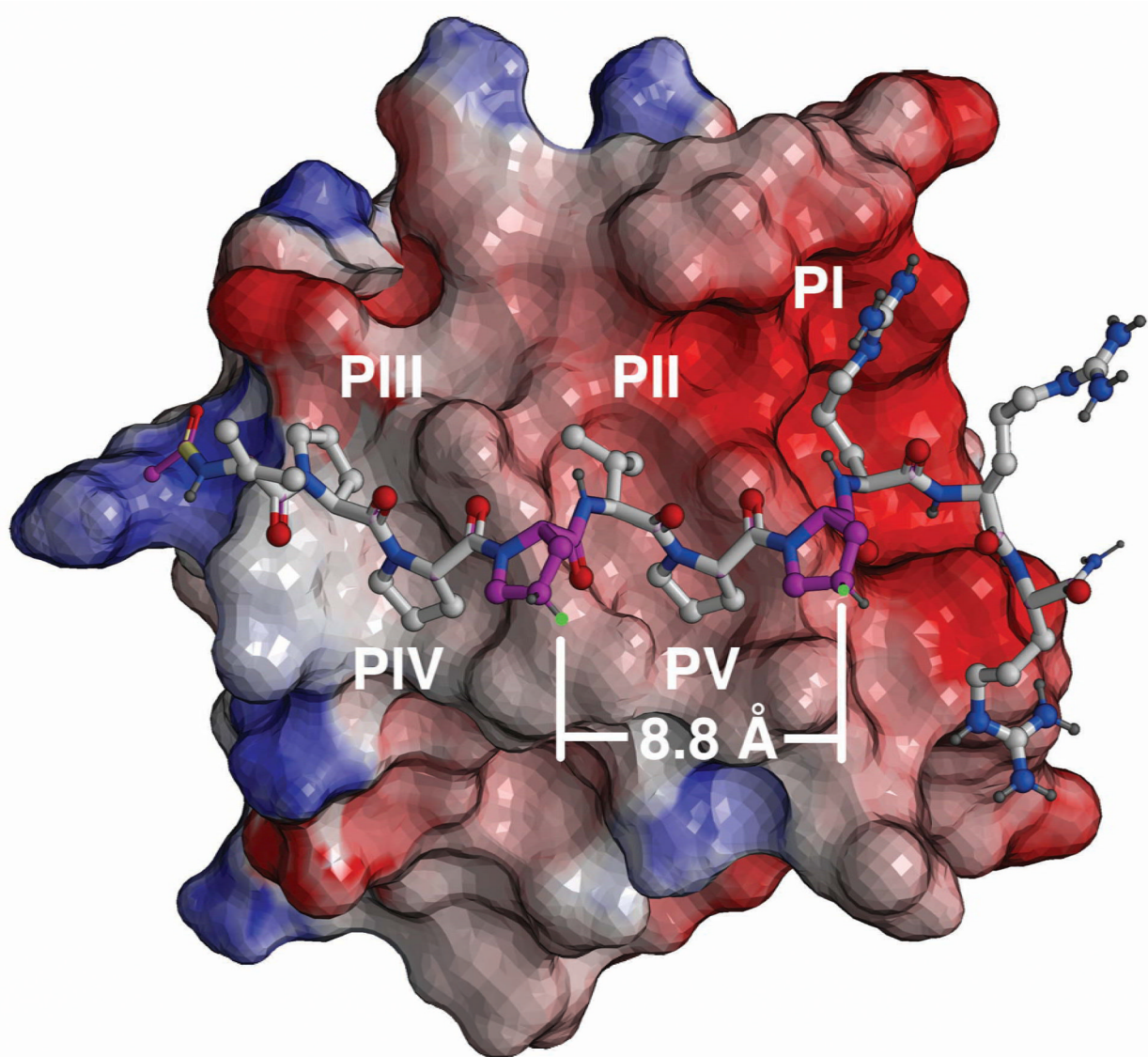
Figure 1.
NMR solution structure of Ac-V-P-P-P-V-P-P-R-R-R-amide (**1**) bound to the Grb2 SH3 N-domain (PDB 3GBQ, reference 32). The peptide binds in a Class II orientation, with interaction pockets identified as PI – PV (reference 28). The protein surface is shown as electrostatic potential (blue – positive; red = negative). Atom coloring: blue = nitrogen; red = oxygen; light grey = carbon and dark grey = hydrogen. Key proline residues of the "P-x-x-P" recognition motif are rendered in solid color (turquoise). Proline residues involved with RCM modification are rendered in magenta, with sites of alkenyloxy attachment shown in green.
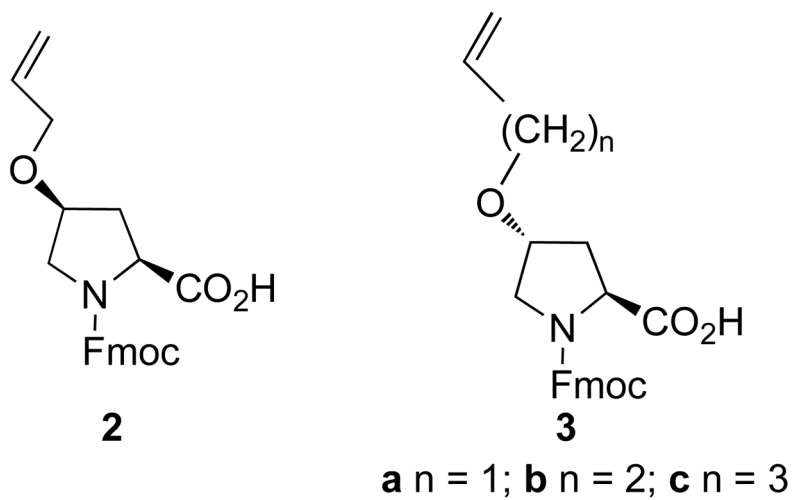
Figure 2.
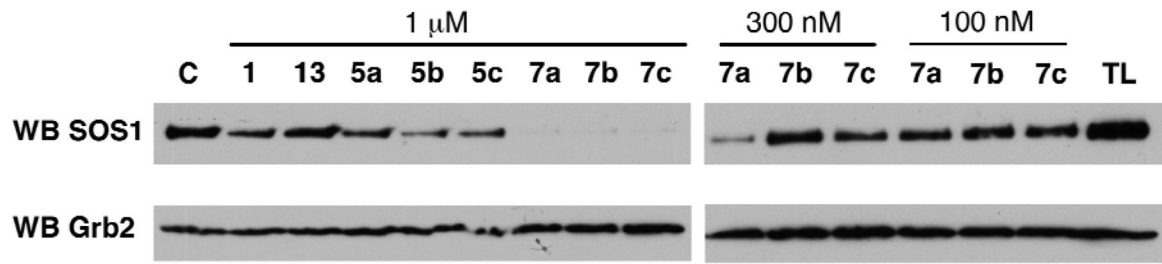Structures of reagents for the solid-phase introduction of alkenyloxy-containing proline residues.

Figure 3.
SDS-PAGE gels showing the effects of synthetic peptides on Grb2-Sos1 association in PC12 cell lysates. Experiments were performed as summarized in the Materials and Methods with protein detection by means of Western blotting. Shown is the amount of Sos1 (top gel) bound to Grb2 (bottom gel) in the presence of the indicated concentrations of peptides. Control (**C**) was run in the absence of peptide with total cell lysate shown as **TL**.
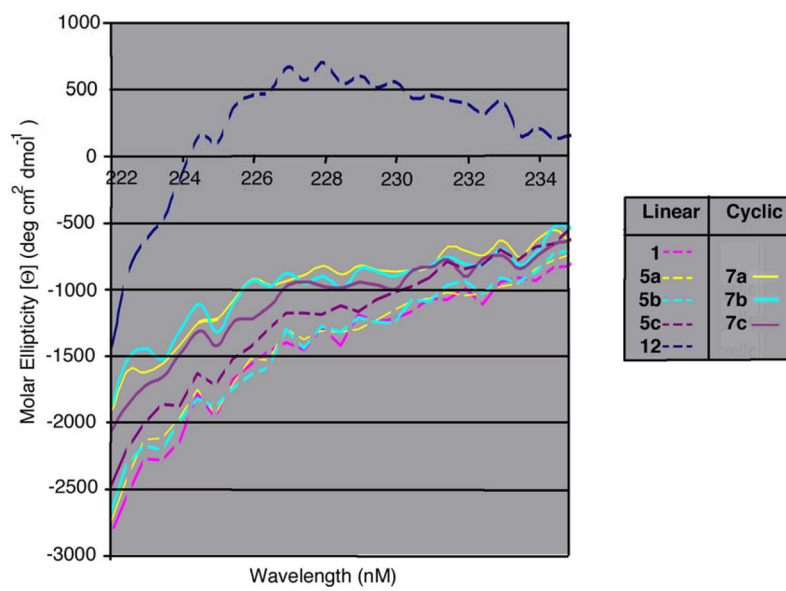
Figure 4.
Expanded CD spectra comparing linear and cyclic peptides.
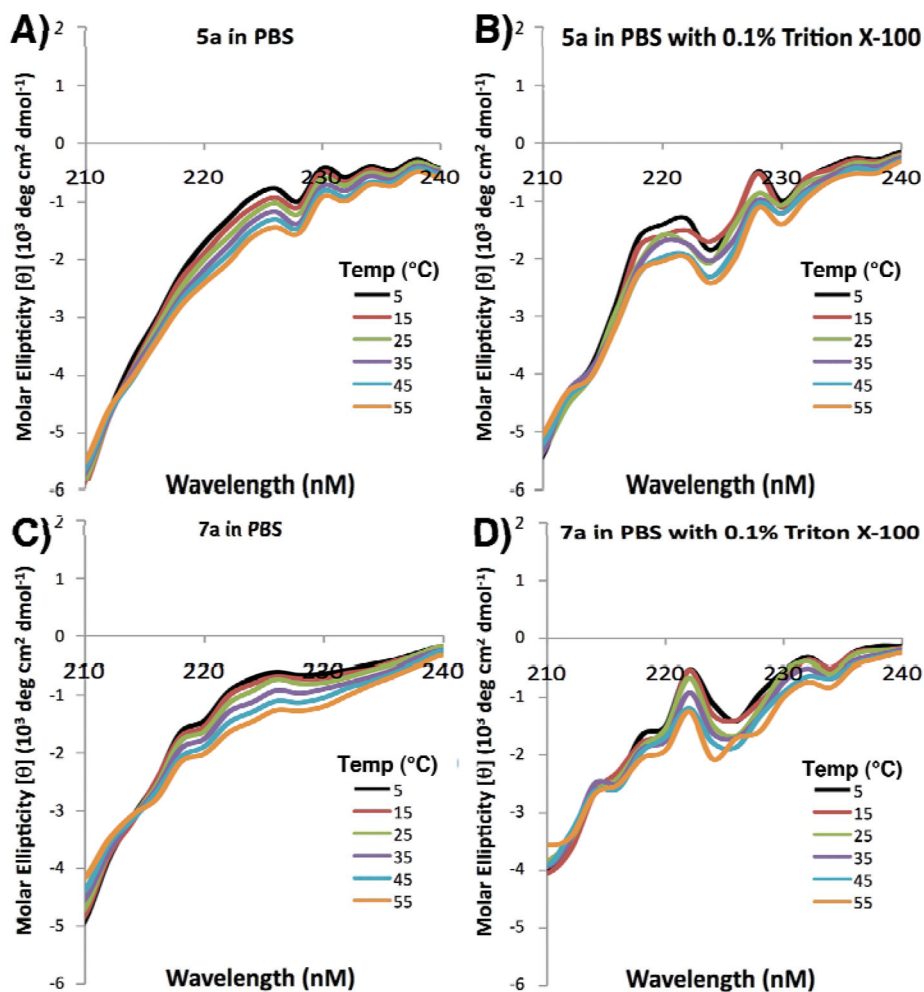
Figure 5.
Far-UV CD run at varying temperatures of peptides **5a** and **7a** in pH 7.4 PBS buffer in the absence (panels **A** nd **C**, respectively) and presence of 0.1% Triton X detergent (Panels **B** and **D**, respectively).
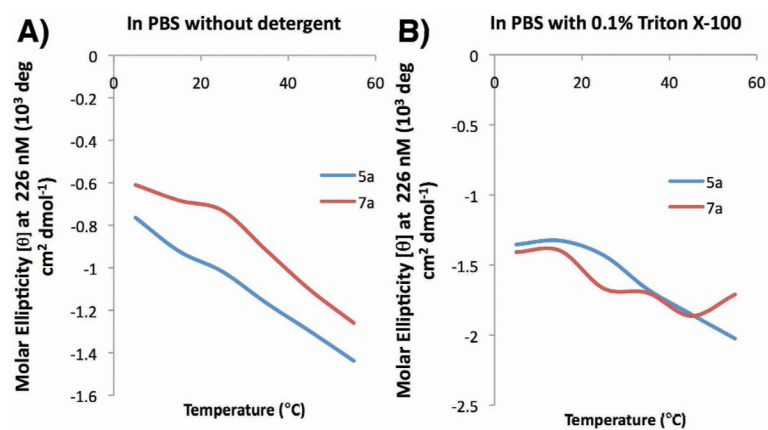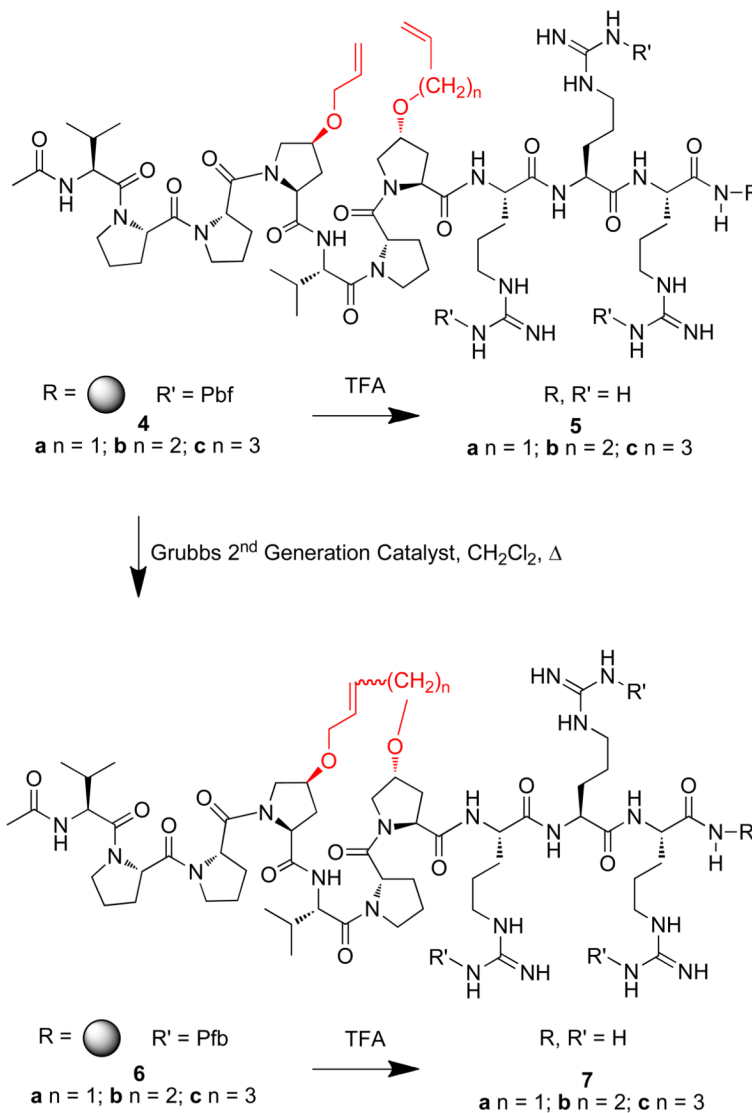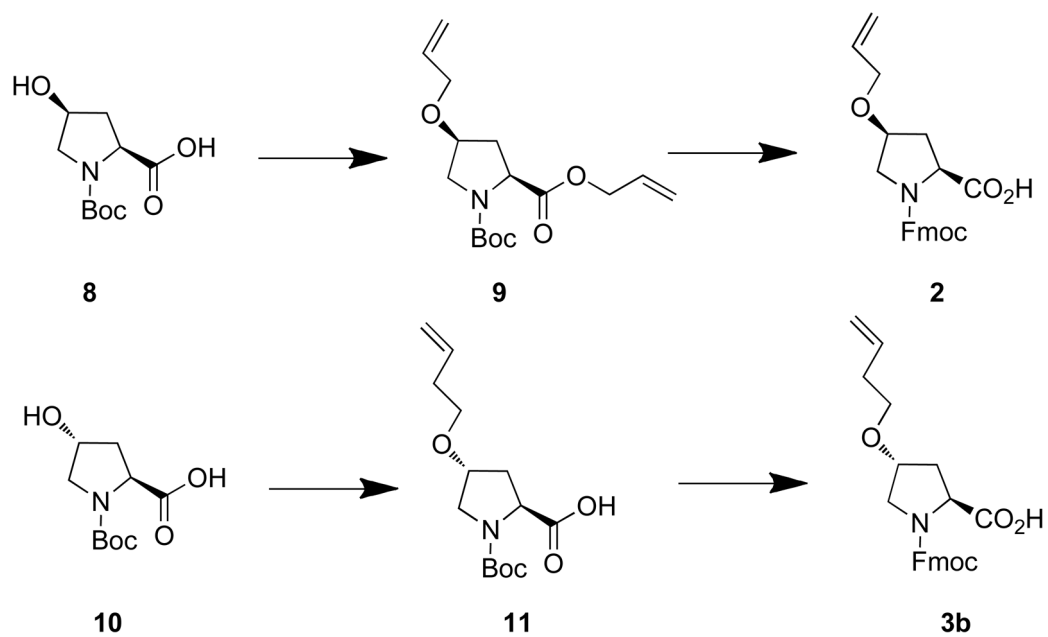
Figure 6.
Change of CD [θ]max = 226 nm as a function of temperature for peptide **5a** and **7a** in pH 7.4 PBS in the absence (panel **A**) and presence (panel **B**) of Triton X detergent.

Scheme 1.
Synthesis peptides described in the text. Shown in red are alkenyloxy groups involved with RCM ring closure.

Scheme 2.
Synthesis of reagents **2** and **3b**.

Table 1

Grb2 SH3 N-Domain in vitro binding affinities[1]

Peptide	$K_d \pm SD$ (μM)[2]
1	11.1 ± 1.31
5a	12.6 ± 0.98
5b	12.2 ± 0.40
5c	14.5 ± 0.75
7a	33.5 ± 1.63
7b	24.2 ± 1.21
7c	18.6 ± 1.11
13	173.1 ± 1.16

[1]Data were obtained using a Trp-fluorescence assay as described in the Materials and Methods.

[2]Dissociation constant ± standard deviation.

Table 2

Peptide ESI Mass Spectral Data.

No	Expected (M + H)$^+$	Observed (M + H)$^+$	HRMS Expected (M + H)$^+$	HRMS Observed (M + H)$^+$
1	1211.7	1211.5		
8	1211.7	1211.7		
9	1207.7	1207.5		
5a	1323.8	1323.8	1323.8008	1323.7892
5b	1337.8	1337.8	1337.8165	1337.8144
5c	1351.8	1351.8	1351.8321	1351.8306
7a	1295.8	1295.8	1295.7695	1295.7672
7b	1309.8	1309.8	1309.7852	1309.7824
7c	1323.8	1323.9	1323.8008	1323.7986